Electronic Supplementary Information

Self-Oriented Sb_2Se_3 Nanoneedle Photocathodes for Water Splitting Obtained by Simple Spin-Coating Method

*Jimin Kim[a†], Wooseok Yang[a†], Yunjung Oh[a], Hyungsoo Lee[a], Seonhee Lee[b], Hyunjung Shin[b], Joosun Kim[c], and Jooho Moon[a]**

[a]Department of Materials Science and Engineering, Yonsei University, 50 Yonsei-ro Seodaemun-gu, Seoul 120-749, Republic of Korea

[b]Department of Energy Science, Sungkyunkwan University, 2066 Seobu-ro, Jangan-gu, Suwon 440-746, Republic of Korea

[c]High-Temperature Energy Materials Research Center, Korea Institute of Science and Technology, Seoul 136-791, Republic of Korea

[†]These authors contributed equally.

**Corresponding author, e-mail: jmoon@yonsei.ac.kr, Tel.: +82-2-2123-2855, Fax: +82-2-312-5375.*

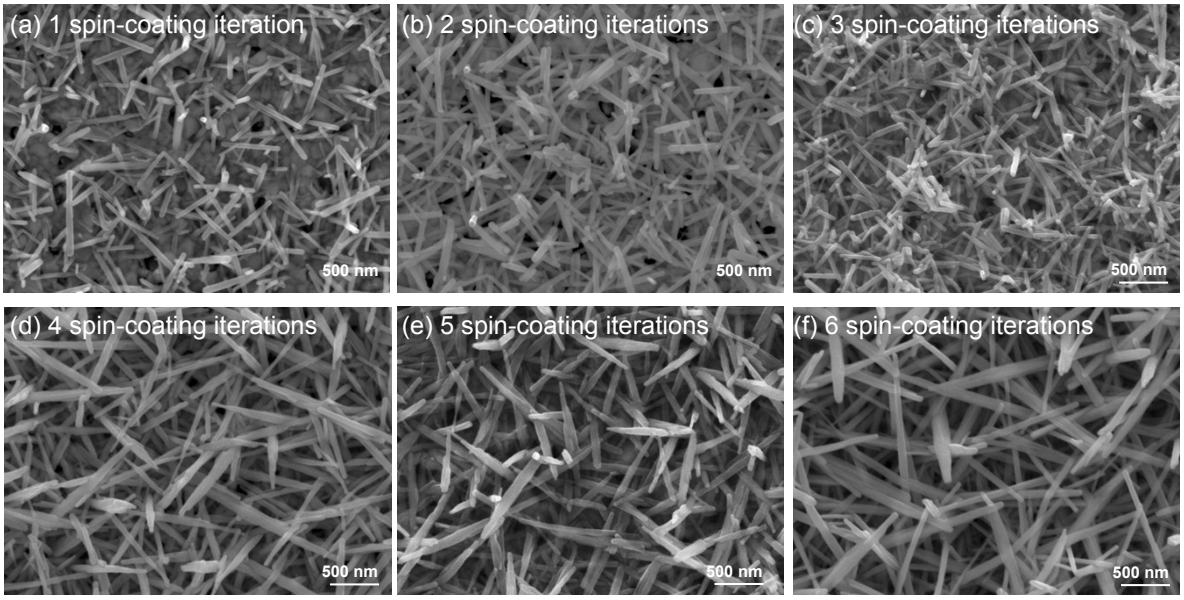

Fig. S1 Top-view SEM images of Sb_2Se_3 nanoneedles after different numbers of spin-coating iterations.

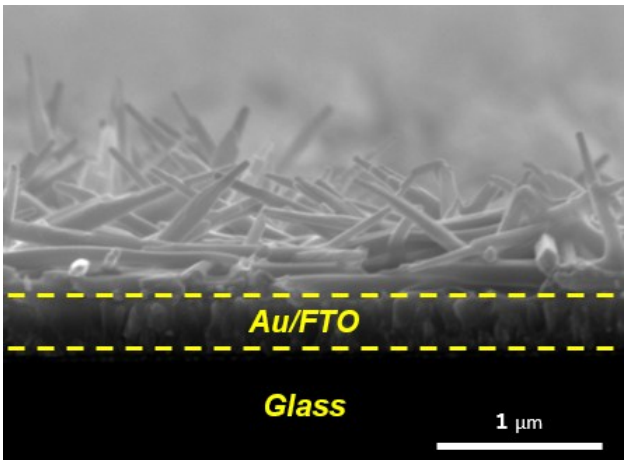

Fig. S2. Cross-sectional SEM image of grass-like Sb_2Se_3 nanoneedle arrays directly grown from the as-spin-coated precursor film.

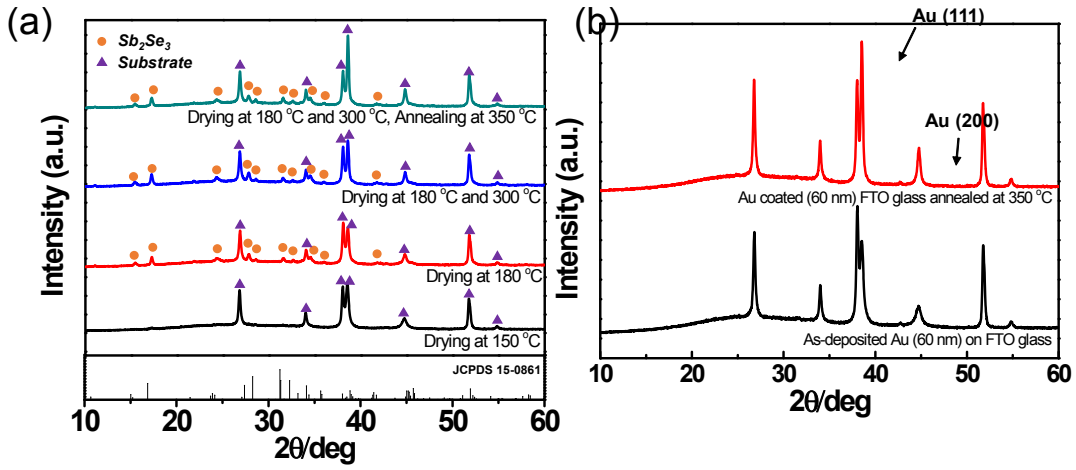

Fig. S3 XRD analysis of (a) Sb_2Se_3/Au (60 nm)/fluorine-doped tin oxide (FTO) as a function of annealing temperature and (b) as-deposited Au (60 nm) on FTO glass and Au-coated (60 nm) FTO glass after annealing at 350 °C.

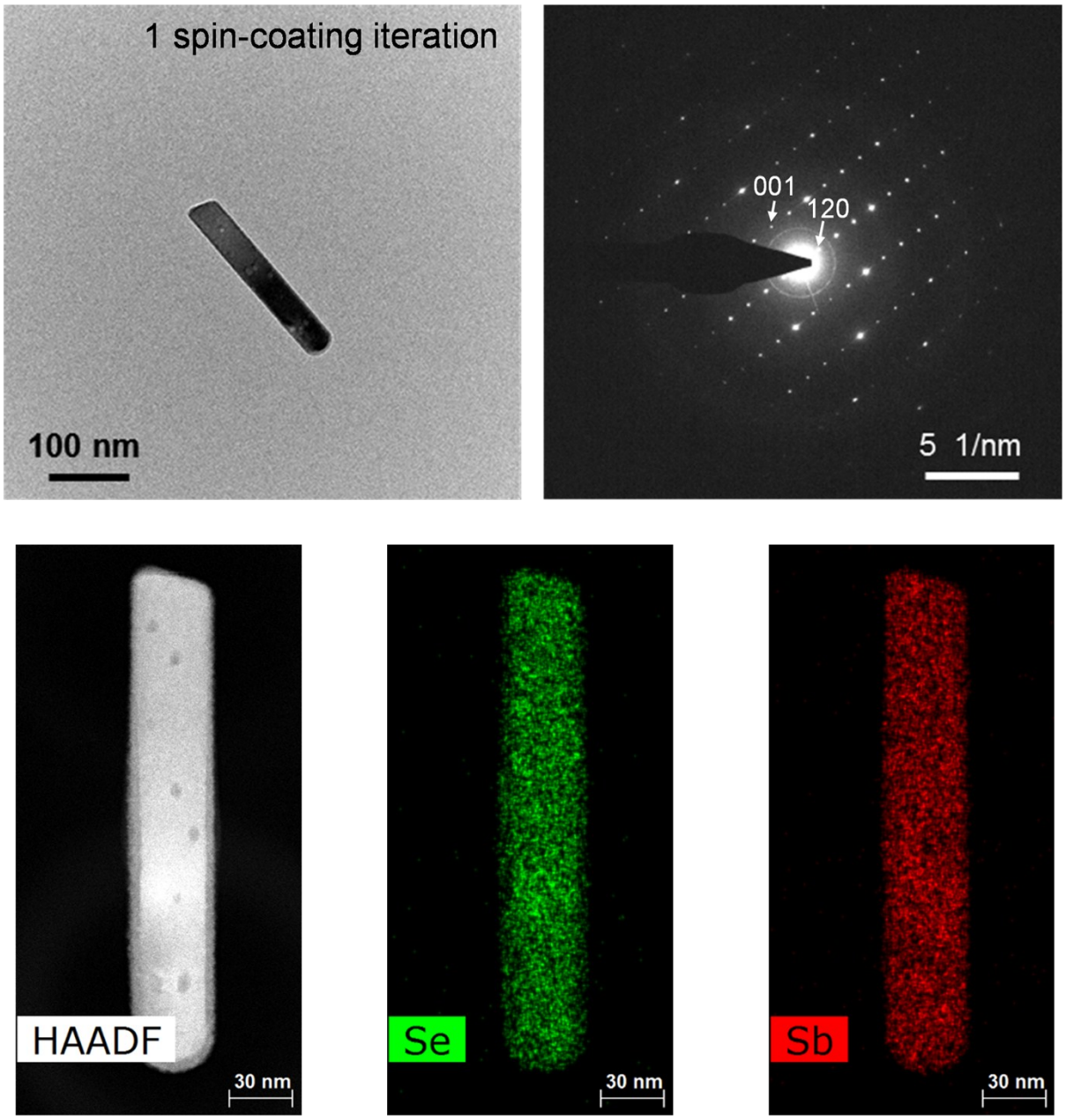

Fig. S4 Low-resolution TEM image and the corresponding selected area electron diffraction (SAED) pattern as well as high-angle annular dark-field (HAADF) and energy-dispersive spectroscopy (EDS) elemental mapping for single Sb_2Se_3 nanorod after one spin-coating iteration.

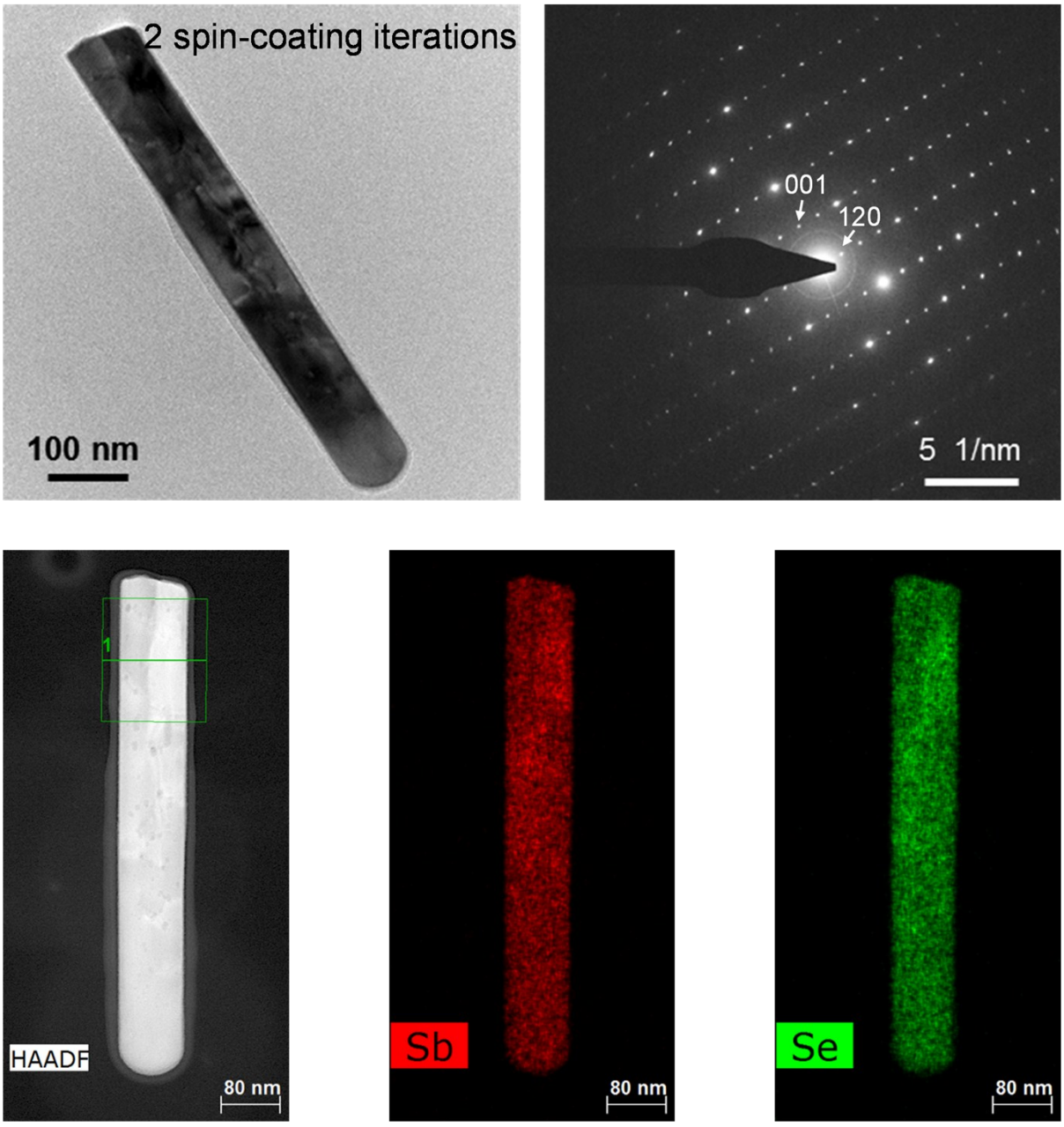

Fig. S5 Low-resolution TEM image and corresponding SAED pattern as well as HAADF and EDS elemental mapping for single Sb_2Se_3 nanorod after two spin-coatings.

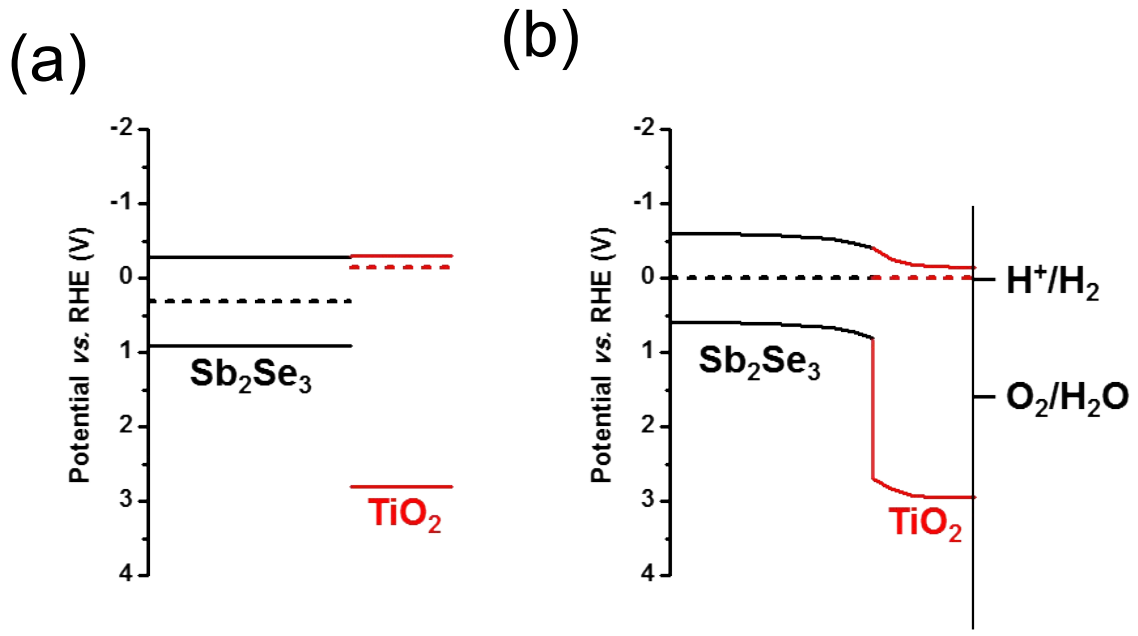

Fig. S6. Schematics of band diagram depicting the energetics of the TiO_2/Sb_2Se_3 photocathode before (a) and after (b) equilibrium in the electrolyte.

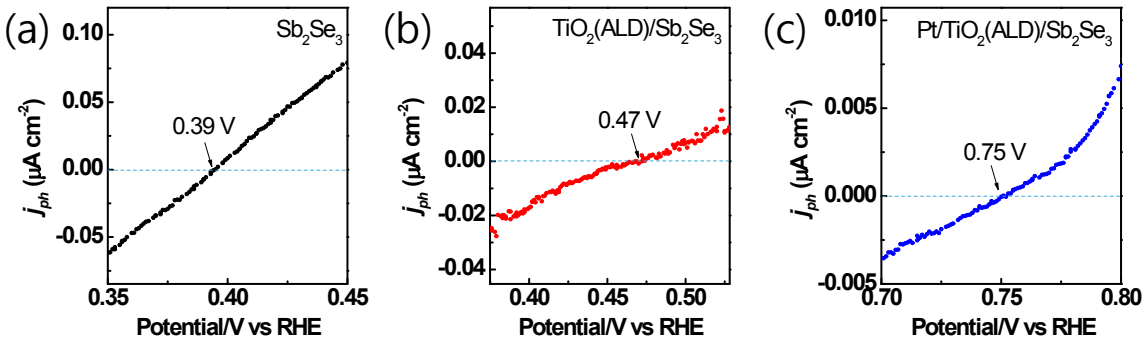

Fig. S7 Onset potential measurement for (a) Sb_2Se_3, (b) TiO_2/Sb_2Se_3, and (c) $Pt/TiO_2/Sb_2Se_3$ determined by obtaining the intercept between the j_{ph} versus E curve and the x axis.

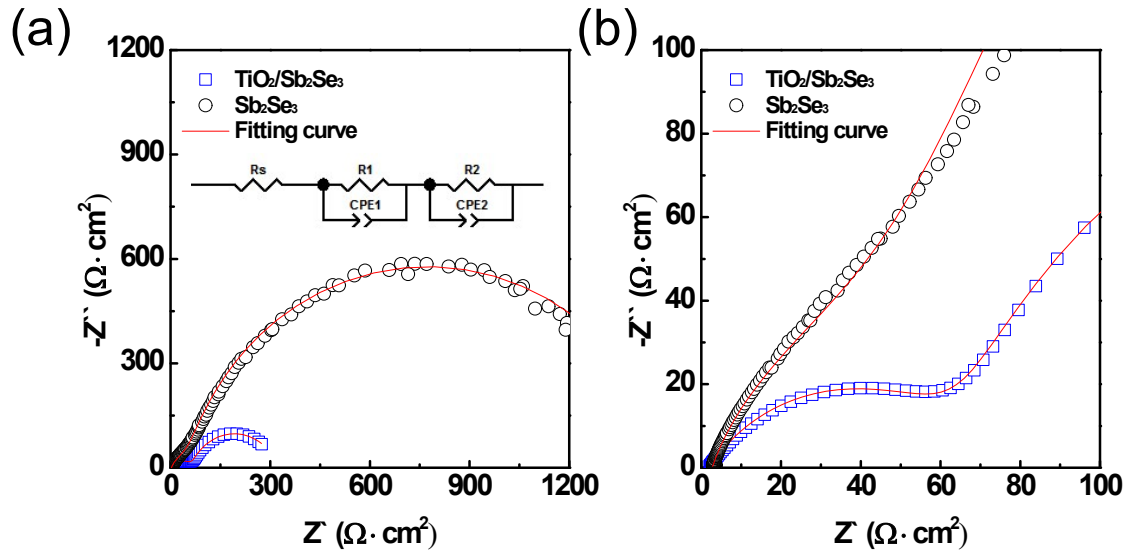

	R_S (Ω cm^{-2})	R_1 (Ω cm^{-2})	CPE$_1$ (F cm^{-2})	R_2 (Ω cm^{-2})	CPE$_2$ (F cm^{-2})
Sb_2Se_3	2.75	48.4	1.39×10^{-4}	1558	1.77×10^{-4}
TiO_2/Sb_2Se_3	2.1	65.1	2.91×10^{-4}	253	3.92×10^{-3}

Fig. S8 Nyquist plots of Sb_2Se_3 and TiO_2/Sb_2Se_3 under simulated solar light illumination: (a) full scale range and (b) enlarged spectra in high-frequency range.

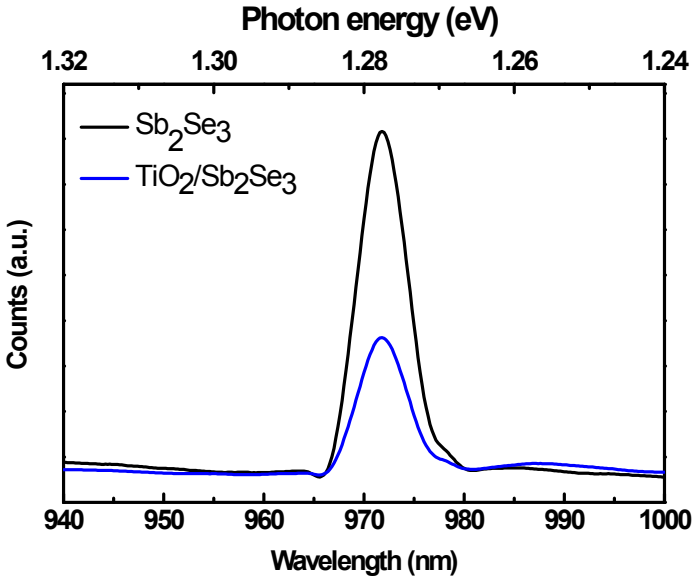

Fig. S9 Photoluminescence emission spectra of Sb_2Se_3 and TiO_2/Sb_2Se_3.

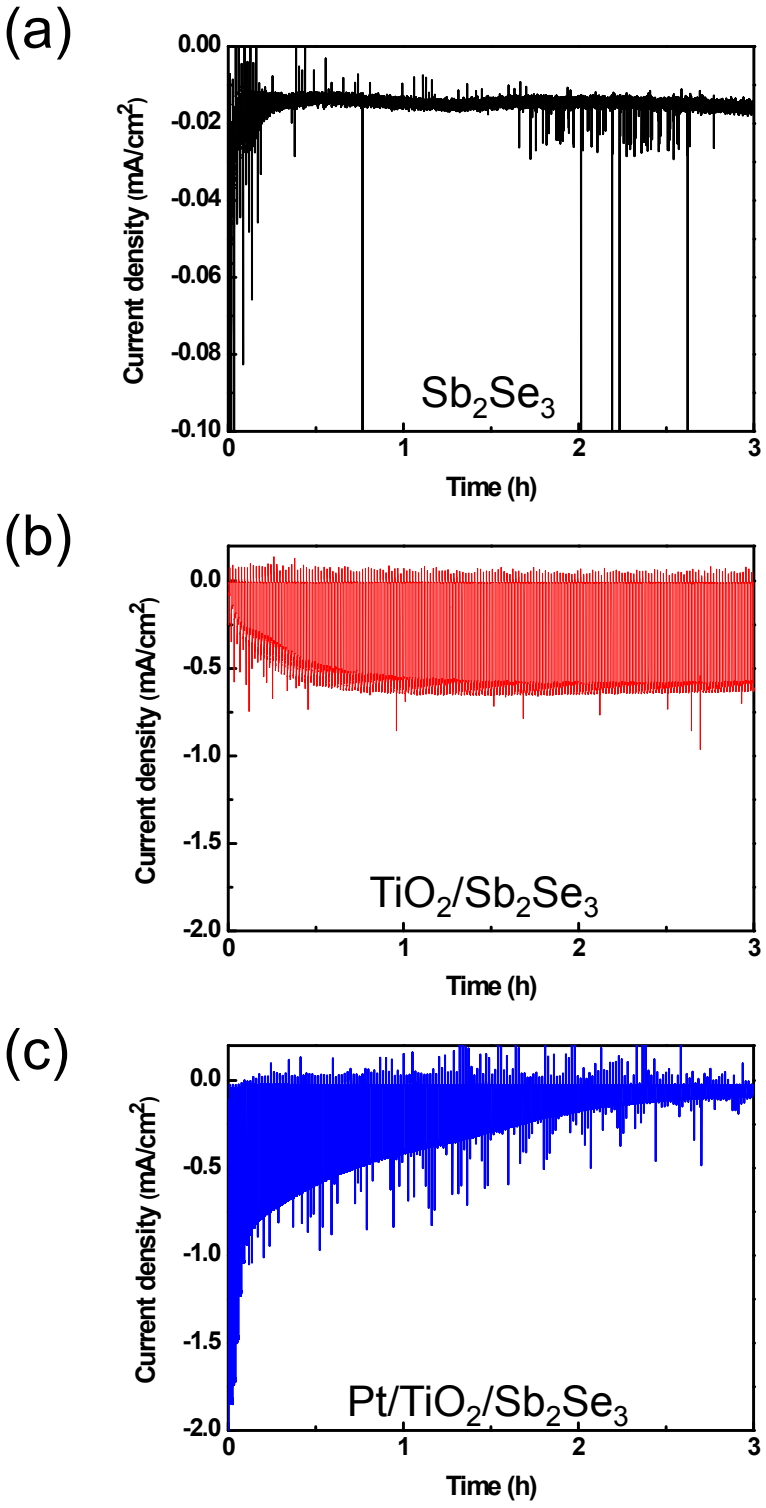

Fig. S10 Current–time curves for (a) Sb_2Se_3, (b) TiO_2/Sb_2Se_3, and (c) $Pt/TiO_2/Sb_2Se_3$ photoelectrodes submerged in 0.5 M H_2SO_4 solution at 0 V_{RHE} under illumination.

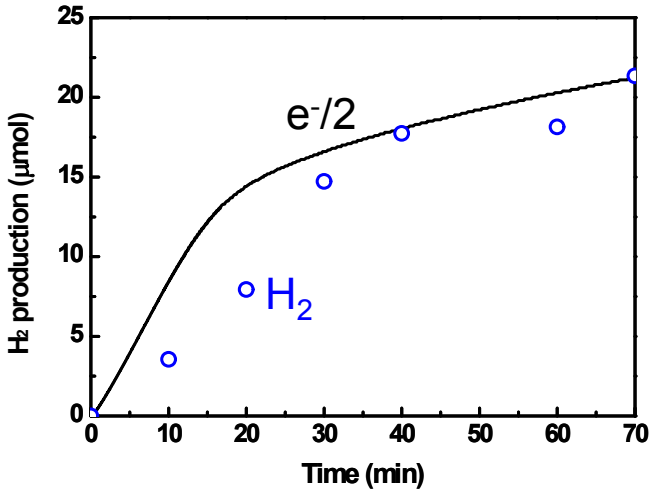

Fig. S11. Time course curve of H_2 evolution over the Pt/TiO_2/Sb_2Se_3 photocathode under simulated sunlight (AM 1.5G) at 0 V vs RHE. The solid line denotes the time course curve for one-half of the electrons passing through the outer circuit ($e^-/2$).